JOURNAL OF SOLID STATE CHEMISTRY 20, 29–41 (1977)

Phase Equilibria in the System V_2O_3–Ti_2O_3–TiO_2 at 1473°K

BORIS BRACH

University of Syktyvkar, October Avenue 55, Syktyvkar 167001, U.S.S.R.

IAN E. GREY AND CHRISTINA LI

CSIRO Division of Mineral Chemistry, P.O. Box 124, Port Melbourne, Victoria 3207, Australia

Received July 19, 1976

The phase equilibria in the V_2O_3–Ti_2O_3–TiO_2 system have been determined at 1473°K by the quench method, using both sealed tubes and controlled gaseous buffers. For the latter, CO_2/H_2 mixtures were used to vary the oxygen fugacity between $10^{-10.50}$ and $10^{-16.73}$ atm. Under these conditions the equilibrium phases are: a sesquioxide solid solution between V_2O_3 and Ti_2O_3 with complete solid solubility and an upper stoichiometry limit of $(V,Ti)_2O_{3.02}$; an M_3O_5 series which has the V_3O_5 type structure between V_2TiO_5 and $V_{0.69}Ti_{2.31}O_5$ and the monoclinic pseudobrookite structure between $V_{0.42}Ti_{2.58}O_5$ and Ti_3O_5; series of Magneli phases, $V_2Ti_{n-2}O_{2n-1}$–Ti_nO_{2n-1}, $n = 4$–8; and reduced rutile phases $(V,Ti)O_{2-x}$, where the lower limit for x is a function of the V/(V + Ti) ratio. The extent of the different solid solution areas and the location of the oxygen isobars have been determined.

1. Introduction

Phase equilibria data in the Fe–V–Ti–O system have an important metallurgical application in the development of processes for treating vanadium-containing iron titanate ore bodies. Australian deposits of vanadiferous titanomagnetites are among the largest in the world and are a potential source of all three metals, iron, titanium, and vanadium. An initial feasibility study on the production of ingot iron, titanium oxide upgrade, and vanadium oxide from the vanadiferous titanomagnetites at Barrambie has already been completed for FerroVanadium Corporation (*1*).

The success of such large scale operations depends largely on the development of suitable economic metallurgical processing methods for separating vanadium, iron and titanium. This in turn requires detailed information on the phase relations and chemical reactions within the system. A proposed processing method (*1*) involves for example electric furnace reduction of ore concentrates to metallic iron plus slags containing high values of titanium and vanadium. The development of this type of process requires a knowledge of the phase equilibria in the Fe–V–Ti–O system under highly reducing conditions. As a first step in the construction of this quaternary system, we have studied the component ternary systems at temperatures and oxygen fugacities considered relevant to commercial reduction processes. Thus, in previous papers we have reported phase relations in the Fe–Ti–O system at 1473°K and for oxygen fugacities in the range 10^{-12}–$10^{-16.5}$ atm (*2*, *3*). In the present study, phase equilibria in the V–Ti–O system have been determined at 1473°K by the quench method using both controlled oxygen fugacity (f_{O_2}) and sealed tube techniques. For the range of oxygen fugacities studied, $10^{-10.5}$ to $10^{-16.7}$ atm, the composition field is bounded by V_2O_3, Ti_2O_3, and TiO_2.

2. Previous Studies

Our present understanding of the complex phase relations in the V_2O_3–VO_2–Ti_2O_3–TiO_2 system is based largely on the pioneering phase characterization work of A. Magneli and co-workers and of G. Andersson in 1954–9 (*4–6*). These workers established the structural basis for homologous series of closely related phases in both the V–O and Ti–O systems, with compositions given by the formulas V_nO_{2n-1}, $4 \leqslant n \leqslant 8$, and Ti_nO_{2n-1}, $4 \leqslant n \leqslant 10$. They also investigated the series $(V,Ti)O_2$, $(V,Ti)_3O_5$ and $(V,Ti)_2O_3$ (*7*). Members of the dioxide series were found to have either the tetragonal rutile structure or a monoclinic distortion of it. In the M_3O_5 series, Ti_3O_5 was found to have two structural modifications (*8*), above and below 460°K, while the structure of V_3O_5 (*9*) was found to be different from either of the Ti_3O_5 types. V_2TiO_5 was also reported to have the V_3O_5 type structure. Recently, Magneli *et al.* (*10*) have shown that there is a third modification of Ti_3O_5, stable between 460°K and 1200°K with a V_3O_5-type structure. Finally, complete solid solubility between V_2O_3 and Ti_2O_3 was observed (*7*). The sesquioxides all have the corundum structure.

There have since been numerous thermodynamic studies on the V–O and Ti–O binary systems, with particular emphasis on the Magneli phases, M_nO_{2n-1}. For the V–O system, the investigations up to 1970 are well referenced in a paper by Okinaka, Kosuge, and Kachi (*11*). These authors determined the oxygen activity of the V_2O_3–VO_2 system in the temperature range 873–1473°K. Above 1273°K a quenching method was applied, varying f_{O_2} with CO_2/H_2 mixtures, while a solid electrolyte cell was used below 1273°K. The only Magneli phases observed were V_4O_7 to V_7O_{13}. Studies on the corresponding Ti–O binary up to 1971 are well documented by Merritt and Hyde (*12*), who carried out an isothermal gravimetric study of the composition range Ti_3O_5 to TiO_2 at 1304°K. In 1972, Suzuki and Sambongi published an extremely comprehensive thermodynamic study on the Ti–O system using EMF measurements with a thoria-based electrolyte and a range of reference electrodes (*13*). Compositions in the range $TiO_{0.6}$ to TiO_2 were investigated in the temperature range 1173–1873°K. More recently, Grey, Li, and Reid have published data on hysteresis in the f_{O_2}–composition isotherms for Ti_nO_{2n-1} Magneli phases (*3*).

Although there is a wealth of information on oxygen activities in the binary systems, there appear to be no published results for any of the ternary solid solutions. In the study reported here, the oxygen fugacity-composition isotherm has been determined at 1473°K for the ternary system V_2O_3–Ti_2O_3–TiO_2.

3. Experimental

3.1. General Procedure

Phase equilibria in the V_2O_3–Ti_2O_3–TiO_2 system at 1473°K were determined by equilibrating weighed mixtures of vanadium and titanium oxides in either controlled gaseous atmospheres or sealed silica tubes, then rapidly quenching the products in liquid nitrogen and determining the phases present and their compositions from chemical and X-ray diffraction analyses. Starting materials were Fisher Certified titanium dioxide (anatase), titanium sesquioxide (Alpha Inorganics, 99.5%), and vanadium sesquioxide, prepared by conversion of the A.R. ammonium vanadate (B.D.H., >99.0%) to V_2O_5 in air at 900°K, followed by reduction in hydrogen at 900°K for 3 h then at 1300°K for 20 h with an intermediate grinding. The TiO_2 was dried at 1000°K prior to use, and the sesquioxides were carefully analysed for small amounts of tetravalent ion for which due allowance was made in the sealed tube studies.

3.2. Gas Equilibration Studies

Up to eight sample pellets, with different $Ti/(Ti + V)$ ratios, were simultaneously equilibrated in flowing gaseous buffers of known oxygen fugacities, for about 50 h. Control of oxygen fugacities was achieved by mixing carbon dioxide and hydrogen in various ratios by use of calibrated flow meters operated at constant pressure. The analytical grade carbon dioxide had a purity of 99.99% ($H_2O < 30$ ppm; air < 100 ppm). The hydrogen used was

of high purity. It was further purified by passage through B.T.S. catalyzer (active copper on alumina substrate) then through molecular sieves.

The equilibration runs were carried out in a horizontal closed-end Alsint alumina tube fitted with a water-cooled quench-end made of brass. This design (*3*), similar to that described by Webster and Bright (*14*), allows efficient preheating of the gas mixture through the inlet tube which extends to the closed end of the work tube. Heat was supplied by a horizontal platinum wound furnace; temperature stability to ±0.5°K was maintained with a Transitrol (Ether Ltd, United Kingdom) potentiometric controller. Temperatures were measured with a calibrated Pt/Pt-13% Rh thermocouple.

The sample pellets were contained in a molybdenum boat fitted with a molybdenum draw wire by which the samples could be rapidly withdrawn from the hot zone. Quenching was facilitated with liquid nitrogen, which was directed onto the sample through ports in the brass quench end.

Further details concerning the experimental apparatus as well as an analysis of the accuracy of results obtained using this method are given in (*3*). The maximum uncertainty in log f_{O_2} is estimated to be ±0.05. A possible source of error in flowing-gas equilibration studies is loss of metal or metal oxide by volatilization. Katsura and Hasegawa (*15*) have previously noted rapid vaporization of vanadium oxides from condensed oxides such as V_6O_{11} and VO_2 at 1600°K. To check the possibility of volatilization under the conditions of our study, we used published thermodynamic data on the V–O system (*16*) to calculate equilibrium fugacities of different vanadium oxide gaseous species above condensed oxides as a function of the oxygen fugacity at 1473°K. The results are presented as plots of log f_{VO_x} vs log f_{O_2} in Fig. 1. Within the oxygen fugacity range of our study, the fugacities of the different gaseous vanadium oxides are all less than 10^{-8} atm. Bearing in mind that these fugacities will be even lower in the ternary V–Ti–O system due to lowering of the activity of the vanadium component phase, it is apparent that volatilization will not be a problem in our studies. The curve for gaseous V_2O_5 (or V_4O_{10}) on the right-hand side of Fig. 1 shows a very rapid rise with increasing oxygen fugacity indicating that volatilization losses above higher condensed oxides such as V_6O_{11} and VO_2 would be severe, as observed experimentally by Katsura and Hasegawa (*15*).

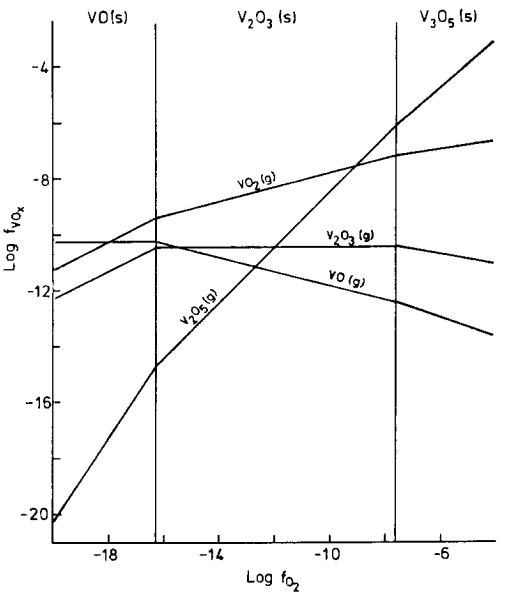

FIG. 1. Thermochemical diagram for the V–O system at 1473°K: fugacities of gaseous VO_x species above solid VO, $VO_{1.5}$, and $VO_{1.67}$ as a function of the oxygen fugacity.

3.3 Sealed Tube Studies

Mixtures of oxides of accurately known stoichiometries were equilibrated in sealed silica tubes then rapidly quenched in liquid nitrogen and the products examined by X-ray diffraction. These studies were used to determine both the extents of the various solid solutions as a function of the V/(V + Ti) ratio and their oxygen stoichiometry ranges. Single phase samples prepared by this method were subsequently used for the determination of lattice parameters by powder X-ray diffraction. Great difficulty was encountered in obtaining structural equilibrium for some of the V_nO_{2n-1}–Ti_nO_{2n-1} solid solutions, and it was necessary to give the samples two or three heat treatments with intermediate grindings.

3.4. *Chemical Analyses*

The oxygen content of the equilibrated samples was determined volumetrically using a method based on the quantitative oxidation of trivalent vanadium and titanium to the tetravalent state with vanadium (V). Thus, the sample was dissolved in a sulphuric acid-hydrofluoric acid solution containing excess pentavalent vanadium while carbon dioxide was bubbled through the solution. The excess vanadium(V) was back titrated with standard ferrous sulphate to determine the number of equivalents, z, of Ti(III) + V(III) in the weight, w, of sample. The oxygen content, y, of the sample $V_aTi_{1-a}O_y$ is determined using the formula

$$y = \frac{2.00w - 23.95z - 1.52az}{w + 8z}.$$

The atomic fraction of vanadium, a, comes from the known molar ratio of oxides in the starting material. As no vaporization occurs, this figure is not expected to change during equilibration. This was confirmed by analyses for total vanadium and titanium on some samples. The method was checked on numerous samples of known oxygen content, prepared by sealed tube reactions. For samples with Ti(III) contents below about 50 wt%, reproducible results were obtained with an accuracy of 2%, corresponding to an error in y of about 0.005. Samples with higher Ti(III) contents were so reducing that they partially decomposed the water. This led to low analyses, the maximum error (determined for Ti_2O_3) being 0.04 in y. For these samples, the oxygen content was determined independently by measuring the weight gain upon oxidation in air at 950°K.

For total vanadium determinations, samples were rendered acid soluble by fusion with sodium bisulphate. Complete oxidation of vanadium to the pentavalent state was effected by addition of potassium permanganate, and the V(V) titrated against standardized ferrous sulphate.

3.5. *X-ray Diffraction*

X-ray powder diffraction patterns were obtained with a Philips diffractometer fitted with a graphite monochromator and using CuKα radiation. Silicon was used as an internal standard for lattice parameter determination, and slow scan rates (0.25°/min) ensured high precision in the data.

4. Results and Discussion

4.1. *Sealed Tube Studies*

The results of sealed-silica tube equilibrations are given in Table I. In these studies extreme difficulty was encountered in obtaining structural equilibrium, particularly in the single phase regions for the solid solutions V_nO_{2n-1}–Ti_nO_{2n-1} with n odd. Whereas analyses on samples equilibrated in controlled gaseous atmospheres showed that chemical equilibrium was generally achieved in a few hours, structural equilibrium could often not be attained even with reaction times which were orders of magnitude greater. However, by repeating the heat treatments with intermediate fine grindings, close approach to structural, as well as chemical, equilibrium was obtained. This is illustrated for many different cases in Table I. For example, a 20 h reaction of a mixture corresponding to the Magneli phase $(V_{0.133}Ti_{0.867})_5O_9$ gave a phase assemblage containing predominantly the two adjacent n-even Magneli phases, $(V,Ti)_4O_7$ and $(V,Ti)_6O_{11}$. This mixture was ground, resealed and reacted for a further 60 h. After this treatment, the quenched products showed M_5O_9 as the major phase but still with significant (>5%) quantities of M_4O_7 and M_6O_{11}. Even a third heat treatment with prior grinding failed to completely eliminate the latter phases. Similar treatments were required to prepare single phase samples of other solid solution series such as $(V,Ti)_3O_5$ and $(V,Ti)_4O_7$. Table I also shows the results for solid solution samples with a fixed V/(V + Ti) metal ratio, in which the oxygen content was varied. Examination of the equilibrated products by X.R.D. for presence of a second phase enabled the oxygen stoichiometry width for the phase to be estimated. The results will be discussed for each of the solid solution series below.

TABLE I

RESULTS OF SEALED SILICA TUBE STUDIES AT 1473°K

Starting composition	Heat treatment	Phases present (by X.R.D.)
$V_{0.97}Ti_{0.03}O_{1.514}$	Single heat for 40 h	α-oxide[a] + V_3O_5 (trace)
$V_{0.90}Ti_{0.10}O_{1.520}$	As above	α-oxide + V_3O_5 (trace)
$V_{0.70}Ti_{0.30}O_{1.520}$	As above	α-oxide + V_3O_5 (trace)
$V_{0.55}Ti_{0.45}O_{1.520}$	Heat for 90 h	α-oxide + V_3O_5 (trace)
$V_{0.40}Ti_{0.60}O_{1.520}$	As above	α-oxide + V_3O_5 (trace)
$V_{0.35}Ti_{0.65}O_{1.530}$	As above	α-oxide + M_3O_5 (minor) + V_3O_5 (minor)
$V_{0.30}Ti_{0.70}O_{1.530}$	As above	α-oxide + M_3O_5 (minor)
$V_{0.10}Ti_{0.90}O_{1.530}$	As above	α-oxide + M_3O_5 (minor)
$TiO_{1.510}$	As above	α-oxide + M_3O_5 (trace)
$TiO_{1.554}$	As above	α-oxide + M_3O_5 (minor)
$V_{0.67}Ti_{0.33}O_{1.660}$	Two heats with intermediate grinding; total 100 h	V_3O_5 + α-oxide (minor)
$V_{0.67}Ti_{0.33}O_{1.667}$	As above	V_3O_5
$V_{0.67}Ti_{0.33}O_{1.674}$	As above	V_3O_5
$V_{0.67}Ti_{0.33}O_{1.680}$	As above	V_3O_5 + M_4O_7 (trace)
$V_{0.60}Ti_{0.40}O_{1.667}$	Heat for 60 h	V_3O_5 + α-oxide (minor) + M_4O_7 (minor)
$V_{0.60}Ti_{0.40}O_{1.667}$	Sample reground and given second heat for 40 h	V_3O_5
$V_{0.50}Ti_{0.50}O_{1.664}$	Two heats with intermediate grinding; total 100 h	V_3O_5 + α-oxide (minor)
$V_{0.50}Ti_{0.50}O_{1.670}$	As above	V_3O_5 + M_4O_7 (trace)
$V_{0.50}Ti_{0.50}O_{1.675}$	As above	V_3O_5 + M_4O_7 (minor)
$V_{0.40}Ti_{0.60}O_{1.667}$	As above	V_3O_5
$V_{0.35}Ti_{0.65}O_{1.667}$	As above	V_3O_5
$V_{0.20}Ti_{0.80}O_{1.667}$	20 h heat	V_3O_5 + M_3O_5 + α-oxide (minor) + M_4O_7 (minor)
$V_{0.20}Ti_{0.80}O_{1.667}$	Sample ground and reheated for 40 h	V_3O_5 + M_3O_5
$V_{0.15}Ti_{0.85}O_{1.667}$	Two heats as above	M_3O_5 + V_3O_5 (minor) + M_4O_7 (trace)
$V_{0.10}Ti_{0.90}O_{1.667}$	Two heats with intermediate ginding; 60 h total	M_3O_5
$V_{0.05}Ti_{0.95}O_{1.667}$	As above	M_3O_5
$V_{0.20}Ti_{0.80}O_{1.667}$	900°C preparation; two 7 day heats with intermediate grinding	α-oxide + M_4O_7
$TiO_{1.667}$	As above	V_3O_5
$V_{0.119}Ti_{0.881}O_{1.739}$	20 h heat	M_4O_7 + V_3O_5 (trace)
$V_{0.095}Ti_{0.905}O_{1.739}$	As above	M_4O_7 + V_3O_5 (trace) + M_3O_5 (faint trace)
$V_{0.071}Ti_{0.929}O_{1.739}$	As above	M_4O_7 + M_3O_5 (trace)
$V_{0.50}Ti_{0.50}O_{1.750}$ ($V_2Ti_2O_7$)	Two heats with intermediate grinding; 60 h total	M_4O_7
$V_{0.35}Ti_{0.65}O_{1.750}$	As above	M_4O_7
$V_{0.20}Ti_{0.80}O_{1.750}$	As above	M_4O_7
$V_{0.125}Ti_{0.875}O_{1.750}$	One heat 40 h	M_4O_7 + V_3O_5 (trace) + M_6O_{11} (trace)

TABLE I—*continued*

Starting composition	Heat treatment	Phases present (by X.R.D.)
$V_{0.100}Ti_{0.900}O_{1.750}$	As above	$M_4O_7 + M_6O_{11}$ (trace) + α-oxide (trace)
$V_{0.075}Ti_{0.925}O_{1.750}$	As above	$M_4O_7 + M_6O_{11}$ (trace)
$V_{0.40}Ti_{0.60}O_{1.80}$ ($V_2Ti_3O_9$)	Two heats with intermediate grinding; total 80 h	M_4O_7, M_6O_{11} Equal amounts + M_5O_9 (faint trace)
$V_{0.267}Ti_{0.733}O_{1.80}$	First heat 20 h	M_4O_7, M_6O_{11} Equal amounts + M_5O_9 (trace) + α-oxide (trace)
$V_{0.267}Ti_{0.733}O_{1.80}$	Sample ground and reheated 100 h	M_4O_7, M_6O_{11} Equal amounts + M_5O_9 (trace)
$V_{0.267}Ti_{0.733}O_{1.80}$	Sample reground and given third heat 20 h	As above with small growth of M_5O_9 relative to M_4O_7 and M_6O_{11}
$V_{0.133}Ti_{0.867}O_{1.80}$	First heat 20 h	M_4O_7, M_6O_{11} Equal amounts + M_5O_9 (minor)
$V_{0.133}Ti_{0.867}O_{1.80}$	Second heat 60 h	M_5O_9 (major) + M_4O_7 (minor) + M_6O_{11} (minor)
$V_{0.133}Ti_{0.867}O_{1.80}$	Third heat 20 h	$M_5O_9 + M_4O_7$ (trace) + M_6O_{11} (trace)
$V_{0.333}Ti_{0.667}O_{1.833}$ ($V_2Ti_4O_{11}$)	Two heats with intermediate grinding; total 100 h	M_6O_{11}
$V_{0.286}Ti_{0.714}O_{1.857}$ ($V_2Ti_5O_{13}$)	As above	M_6O_{11}, M_8O_{15} Equal amounts + M_7O_{13} (trace)
$V_{0.25}Ti_{0.75}O_{1.875}$ ($V_2Ti_6O_{15}$)	As above	M_8O_{15} (major) + M_6O_{11} (minor) + MO_{2-x} (minor)
$V_{0.04}Ti_{0.96}O_{1.98}$	One heat, 40 h	Rutile + MO_{2-x} (minor)
$V_{0.02}Ti_{0.98}O_{1.99}$	As above	Rutile
$TiO_{1.98}$	As above	Rutile + TiO_{2-x} (minor)
$TiO_{1.99}$	As above	Rutile

[a] Nomenclature for phases is consistent with previous use (*2*), i.e., α-oxide refers to a solid solution with composition M_2O_3, possessing the corundum structure, M_3O_5 refers to a solid solution with the pseudobrookite structure. Magneli phases are represented by M_nO_{2n-1} and other reduced rutile phases by MO_{2-x}. V_3O_5 refers to a $(V,Ti)_3O_5$ solid solution with the V_3O_5 structure.

4.2. Gas Equilibration Studies

The results of the controlled oxygen fugacity studies are given in Table II and plotted as oxygen isobars in the V_2O_3–Ti_2O_3–TiO_2 composition plane in Fig. 2. In addition to chemical analyses, X-ray diffraction studies on α-oxides were used to locate the positions of the oxygen fugacity lines in Fig. 2; i.e. accurate lattice parameters were obtained for α-oxide phases when present in the equilibrated samples, and the compositions measured off a lattice parameter vs composition curves (Fig. 3). For the case of the other $(V,Ti)_nO_{2n-1}$ solid solutions, the changes of lattice parameters with composition were generally too small for use of this approach accurately. The V_2O_3–Ti_2O_3–TiO_2 system contains two invariants, for which the oxygen fugacities

TABLE II

RESULTS OF CONTROLLED ATMOSPHERE QUENCH STUDIES ON THE V_2O_3–Ti_2O_3–TiO_2 SYSTEM AT 1473°K

Logf_{O_2}	Starting mixture (moles) $VO_{1.5}$	Starting mixture (moles) TiO_2	O/(V + Ti) in equilibration product	Phases present in equilibrium mixture (by X.R.D.)
−10.50	0.90	0.10	1.530	α-oxide (major) + V_3O_5 (minor)
	0.70	0.30	1.657	V_3O_5 (major) + α-oxide (minor)
	0.414	0.586	1.785	M_4O_7 + M_5O_9
	0.264	0.736	1.856	M_6O_{11} + M_7O_{13} + M_8O_{15}
	0.082	0.918	1.947	Rutile + MO_{2-x}
−12.20	0.90	0.10	1.504	α-oxide
	0.80	0.20	1.556	α-oxide (major) + V_3O_5 (minor)
	0.70	0.30	1.623	α-oxide (minor) + V_3O_5 (major)
	0.516	0.484	1.702	V_3O_5 + M_4O_7
	0.416	0.584	1.754	M_4O_7 + M_5O_9 (trace)
	0.347	0.653	1.790	M_4O_7 + M_6O_{11} + M_5O_9 (trace)
	0.263	0.737	1.829	M_6O_{11} + M_4O_7 (minor) + M_7O_{11} (minor) + M_8O_{15} (minor)
	0.151	0.849	1.896	MO_{2-x}
	0.082	0.918	1.934	MO_{2-x} + rutile (minor)
	0.062	0.938	1.950	Rutile + MO_{2-x}
−13.73	0.512	0.488	1.650	V_3O_5 + α-oxide (minor)
	0.347	0.653	1.743	M_4O_7 + V_3O_5 (minor) + α-oxide (trace)
	0.211	0.789	1.828	M_6O_{11} + M_4O_7 (minor)
	0.062	0.938	1.922	MO_{2-x}
	0.00	1.00	1.992	Rutile
−15.00	0.512	0.488	1.575	α-oxide + V_3O_5 (minor)
	0.440	0.560	1.623	α-oxide + V_3O_5
	0.389	0.611	1.659	V_3O_5 + α-oxide + M_4O_7 (minor)
	0.347	0.653	1.681	V_3O_5 + M_4O_7 (minor) + α-oxide (minor)
	0.265	0.735	1.726	M_4O_7 + V_3O_5 + α-oxide (minor)
	0.211	0.789	1.753	M_4O_7 + M_5O_9 (trace) + α-oxide (trace)
	0.118	0.882	1.809	M_4O_7 + M_5O_9 + M_6O_{11}
	0.118	0.882	1.801	As above
	0.082	0.918	1.839	M_6O_{11} + M_4O_7 (trace) + M_5O_9 (trace)
	0.082	0.918	1.827	As above
	0.000	1.000	1.876	Ti_8O_{15}
−15.80	0.438	0.562	1.543	α-oxide + V_3O_5 (minor)
	0.389	0.611	1.590	α-oxide + V_3O_5
	0.264	0.736	1.669	V_3O_5 + M_4O_7 + α-oxide
	0.118	0.882	1.738	M_4O_7 + V_3O_5 (trace) + α-oxide (trace)
	0.082	0.918	1.749	M_4O_7 + M_5O_9 (trace) + α-oxide (trace)
	0.000	1.000	1.801	Ti_5O_9

TABLE II—*continued*

Logf_{O_2}	Starting mixture (moles) $VO_{1.5}$	Starting mixture (moles) TiO_2	O/(V + Ti) in equilibration product	Phases present in equilibrium mixture (by X.R.D.)
−15.85	0.512	0.488	1.513	α-oxide
	0.347	0.653	1.610	V_3O_5 + α-oxide
	0.211	0.789	1.692	V_3O_5 + M_4O_7 (minor) + α-oxide (minor)
	0.062	0.938	1.749	M_4O_7 + V_3O_5 (trace) + α-oxide (trace)
	0.000	1.000	1.802	Ti_5O_9 + Ti_4O_7 (trace)
−16.25	0.300	0.700	1.615	α-oxide + V_3O_5
	0.200	0.800	1.674	α-oxide + V_3O_5 + M_4O_7
	0.100	0.900	1.729	M_4O_7 + V_3O_5 (minor) + α-oxide (minor)
	0.082	0.918	1.722	M_4O_7 + M_3O_5 + V_3O_5 (trace) + α-oxide (trace)
	0.062	0.938	1.736	M_4O_7 + M_3O_5 (minor)
	0.000	1.000	1.754	Ti_4O_7
−16.50	0.389	0.611	1.530	α-oxide + V_3O_5 (trace)
	0.265	0.735	1.639	α-oxide + M_3O_5 + V_3O_5 (minor)
	0.118	0.882	1.702	M_3O_5 + M_4O_7 (minor) + α-oxide (minor)
	0.082	0.918	1.714	M_3O_5 + M_4O_7
	0.062	0.938	1.743	M_4O_7 + M_3O_5 (minor)
	0.000	1.000	1.752	Ti_4O_7
−16.73	0.415	0.585	1.511	α-oxide
	0.300	0.700	1.589	α-oxide + V_3O_5 (minor)
	0.200	0.800	1.644	α-oxide + V_3O_5 + M_3O_5
	0.100	0.900	1.672	M_3O_5 + V_3O_5 (trace) + α-oxide (trace)
	0.062	0.938	1.668	M_3O_5
−17.40	0.347	0.653	1.511	α-oxide
	0.300	0.700	1.532	α-oxide + M_3O_5 (trace)
	0.200	0.800	1.610	α-oxide + M_3O_5
	0.100	0.900	1.665	α-oxide (minor) + M_3O_5
	0.000	1.000	1.669	Ti_3O_5

and phase compositions are listed in Table III. Both three-phase assemblages occur at very low oxygen fugacities, which require hydrogen and carbon dioxide gas flows which are close to the practical limits which can be achieved with our apparatus. The logf_{O_2} values given in Table III must thus be viewed with caution, as their associated error is of the order of 0.2.

4.3. α-Oxide Solid Solution

Complete mutual solubility of V_2O_3 and Ti_2O_3 has been established in earlier studies (*7*), and in our study we find no evidence of a miscibility gap at 1473°K. From sealed tube studies and chemical analyses on gas-equilibrated samples we find that members of the α-oxide series have a small range of oxygen nonstoichiometry due to incorporation of excess oxygen. The extent of incorporation is approximately constant along the series at ~2 mol%, corresponding to an upper composition limit of $(V,Ti)O_{1.51}$. Magneli *et al.* have previously determined the same upper limit for the titanium end member, i.e. $TiO_{1.51}$ (*5*).

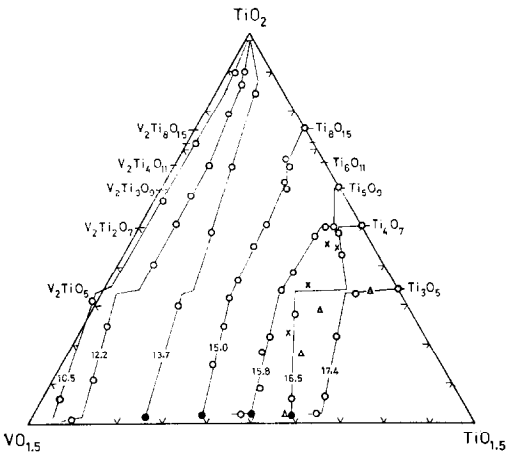

FIG. 2. Oxygen isobars in the V_2O_3–Ti_2O_3–TiO_2 system at 1473°K (compositions in mol%). Numbers on the lines are values of $-\log f_{O_2}$. o, experimental data from chemical analyses on quenched samples; ●, data obtained using lattice parameter-composition relationships; ×, points for $f_{O_2} = 10^{-16.25}$; △, points for $f_{O_2} = 10^{-16.73}$. The offsets in the isobars occur at phase boundaries, which have been omitted for clarity (see, however, Fig. 5).

We reacted a series of α-oxide compositions with $O/(V + Ti) > 1.51$ in sealed silica tubes to obtain α-oxide solid solution members along the upper stoichiometry boundary, together with a small amount of $(V,Ti)_3O_5$ in each case. Lattice parameters were determined for these phases and are listed in Table IV and plotted in Fig. 3. The change in the unit cell parameters with oxygen content is given in Table IV for the end member compositions. Whereas the titanium end member undergoes a hexagonal *c*-axis expansion of 0.04 Å from $TiO_{1.50}$ to $TiO_{1.51}$, the vanadium end member suffers a contraction in the c parameter upon incorporation of TiO_2. These results illustrate how important it is to allow for the effects of oxygen-nonstoichiometry when preparing calibration curves for the determination of compositions from lattice parameter measurements. Obviously, different curves are needed for the determination of compositions of α-oxide phases in assemblages containing $(V,Ti)_3O_5$ as a second phase, cf. assemblages with (V,Ti)O as the second phase.

The α-oxide composition $V_{0.76}Ti_{1.24}O_{3.02}$ coexists with both M_3O_5 and V_3O_5 phases at

TABLE III

INVARIANT POINTS IN THE SYSTEM V_2O_3–Ti_2O_3–TiO_2 AT 1473°K

Log f_{O_2}	Phases present	Compositions
−16.25	M_4O_7	$V_{0.32}Ti_{3.68}O_7$
	+	
	M_3O_5	$V_{0.42}Ti_{2.58}O_{5.02}$
	+	
	V_3O_5	$V_{0.69}Ti_{2.31}O_{5.02}$
−16.73	α-oxide	$V_{0.76}Ti_{1.24}O_{3.02}$
	+	
	M_3O_5	$V_{0.42}Ti_{2.58}O_{5.00}$
	+	
	V_3O_5	$V_{0.69}Ti_{2.31}O_{5.00}$

an oxygen fugacity of $10^{-16.73}$ atm at 1473°K. Oxidation of α-oxides with lower $V/(V + Ti)$ ratios give M_3O_5 compositions, whereas α-oxides with higher $V/(V + Ti)$ ratios may be oxidized to V_3O_5 type phases.

4.4. *V_2TiO_5–Ti_3O_5 Solid Solution*

Earlier work by Magneli *et al.* (*7*) showed that V_2TiO_5 was isostructural with V_3O_5 (*9*). Our studies at 1473°K are consistent with the V_3O_5 structure type persisting with increasing titanium content up to a limiting composition $V_{0.69}Ti_{2.31}O_5$. For compositions between $V_{0.69}Ti_{2.31}O_5$ and $V_{0.42}Ti_{2.58}O_5$ the V_3O_5 structure type coexists with a M_3O_5 phase isostructural with Ti_3O_5. The structure of the latter phase may be described as a monoclinic distortion of the pseudobrookite structure (*8*). This structure type is stable for M_3O_5 compositions between $V_{0.42}Ti_{2.58}O_5$ and Ti_3O_5.

Lattice parameters for the V_3O_5 and M_3O_5 solid solutions are given in Table IV. The data for the V_3O_5 series are plotted in Fig. 4. Included in this diagram are points for V_3O_5 (*9*) and Ti_3O_5 (*10*). The latter compound exists as a V_3O_5-structure modification between 460°K and 1200°K (*10*). It is apparent from Fig. 4 that quite marked changes in the lattice parameter-composition curves occur near the compositions V_2TiO_5 and VTi_2O_5. Further data for compositions with $V/(V + Ti)$ ratios between 0.67 and 1.0 and between 0.008 and 0.25 are needed.

TABLE IV

LATTICE PARAMETERS FOR VARIOUS V_nO_{2n-1}–Ti_nO_{2n-1}, $n = 2$–4, SOLID SOLUTIONS (STANDARD DEVIATIONS GIVEN IN PARENTHESES)

Composition	Structure type and symmetry	Lattice parameters						References
		a(Å)	b(Å)	c(Å)	α(°)	β(°)	γ(°)	
$VO_{1.500}$	Corundum rhombohedral (hexagonal constants given)	4.9491(2)		13.998(1)				*20*
$V_{0.97}Ti_{0.03}O_{1.51}$	As above	4.9599(7)		13.985(2)				This work
$V_{0.90}Ti_{0.10}O_{1.51}$	As above	4.9733(9)		13.986(2)				This work
$V_{0.70}Ti_{0.30}O_{1.51}$	As above	4.9910(6)		13.988(2)				This work
$V_{0.55}Ti_{0.45}O_{1.51}$	As above	5.0094(5)		13.980(1)				This work
$V_{0.40}Ti_{0.60}O_{1.51}$	As above	5.0321(6)		13.957(2)				This work
$V_{0.30}Ti_{0.70}O_{1.51}$	As above	5.0484(8)		13.946(2)				This work
$V_{0.10}Ti_{0.90}O_{1.51}$	As above	5.0940(4)		13.834(1)				This work
$TiO_{1.500}$	As above	5.155		13.607				*21*
$TiO_{1.51}$	As above	5.1451(4)		13.639(1)				This work
$VO_{1.667}$	V_3O_5 type monoclinic	10.005(1)	5.0416(5)	9.859(1)		138.80(1)		*10*
$V_{0.67}Ti_{0.33}O_{1.660}$	As above	10.084(4)	5.067(2)	9.960(4)		139.03(1)		This work
$V_{0.67}Ti_{0.33}O_{1.674}$	As above	10.081(4)	5.066(2)	9.955(3)		139.03(1)		This work
$V_{0.67}Ti_{0.33}O_{1.680}$	As above	10.074(5)	5.064(2)	9.953(5)		139.03(1)		This work
$V_{0.60}Ti_{0.40}O_{1.667}$	V_3O_5 type monoclinic	10.084(4)	5.062(2)	9.966(4)		138.99(1)		This work
$V_{0.50}Ti_{0.50}O_{1.664}$	As above	10.087(4)	5.056(2)	9.976(4)		138.80(1)		This work
$V_{0.50}Ti_{0.50}O_{1.670}$	As above	10.081(4)	5.057(2)	9.974(4)		138.83(1)		This work
$V_{0.50}Ti_{0.50}O_{1.675}$	As above	10.081(3)	5.058(2)	9.970(3)		138.85(1)		This work
$V_{0.40}Ti_{0.60}O_{1.667}$	As above	10.085(4)	5.054(2)	9.981(4)		138.70(1)		This work
$V_{0.25}Ti_{0.75}O_{1.667}$	As above	10.086(4)	5.055(2)	9.981(4)		138.53(1)		This work
$TiO_{1\ 667}$	As above	10.120(2)	5.074(1)	9.070(2)		138.15(1)		This work
$TiO_{1.667}$	Pseudobrookite monoclinic	9.82	3.78	9.97		91.0		*8*
$V_{0.062}Ti_{0.938}O_{1.667}$	As above	9.823(2)	3.782(1)	9.959(2)		91.00(2)		This work
$V_{0.082}Ti_{0.918}O_{1.667}$	As above	9.817(2)	3.777(1)	9.953(2)		90.93(1)		This work
$V_{0.118}Ti_{0.882}O_{1.667}$	As above	9.821(4)	3.771(1)	9.920(4)		90.88(2)		This work
$V_{0.50}Ti_{0.50}O_{1.75}$	M_4O_7 triclinic	5.583(2)	7.030(2)	12.408(3)	94.93(1)	95.05(1)	108.57(1)	This work
$V_{0.35}Ti_{0.65}O_{1.75}$	As above	5.594(2)	7.063(2)	12.420(4)	95.05(1)	95.07(1)	108.76(2)	This work
$V_{0.20}Ti_{0.80}O_{1.75}$	As above	5.587(2)	7.095(2)	12.420(4)	95.03(1)	95.12(1)	108.66(2)	This work
$TiO_{1.75}$	As above	5.593(1)	7.119(1)	12.452(3)	95.06(1)	95.12(1)	108.75(1)	This work

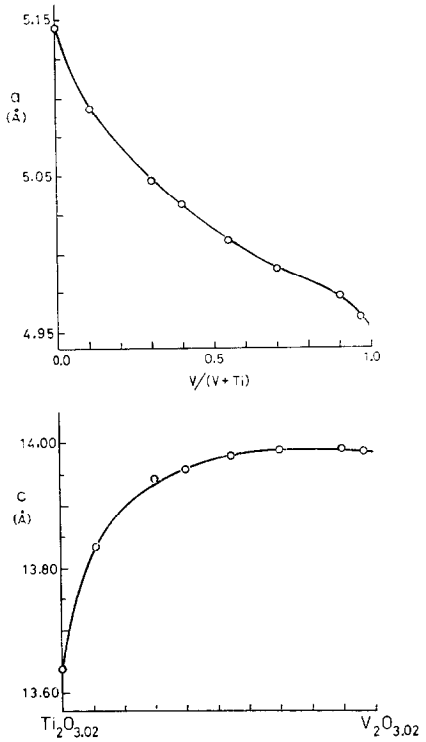

FIG. 3. Variation of lattice parameters with composition for members of the α-oxide series in equilibrium with $(V,Ti)_3O_5$ phases. The α-oxide phases are oxygen-rich with compositions $V_xTi_{1-x}O_{1.500+\delta}$, $\delta \simeq 0.01$.

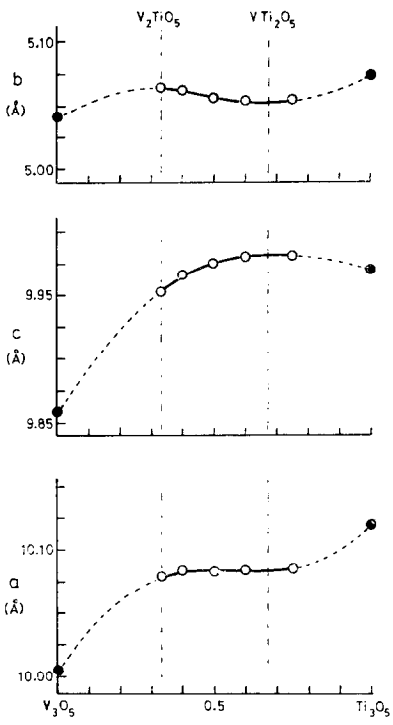

FIG. 4. Variation of lattice parameters with composition in the series V_3O_5–Ti_3O_5, with V_3O_5 type structure.

The oxygen stoichiometry range for the V_2TiO_5–Ti_3O_5 series was studied on samples reacted in sealed tubes. The results are given in Table I. The boundaries were determined from the appearance of a second phase in the X-ray diffractograms. The accuracy of this method was checked on a series of standard mixtures containing known weights of $(V,Ti)_3O_5$ and $(V,Ti)_4O_7$ or $(V,Ti)_2O_3$. The lower limit of detection of α-oxide and M_4O_7 by X.R.D. was ~2 and 5 wt% respectively, corresponding to ~0.004 in the O/(V + Ti) atomic ratio. $(V,Ti)_3O_5$ phases in equilibrium with α-oxide were observed to have the stoichiometric O/(V + Ti) value of 1.667, whereas the phases in equilibrium with M_4O_7 were oxygen rich, the amount increasing with increasing vanadium content to a maximum value of O/(V + Ti) = 1.675 for a V/(V + Ti) ratio of 0.67. Lattice parameters for $V_{0.67}Ti_{0.33}O_y$ and $V_{0.50}Ti_{0.50}O_y$ as a function of y are given in Table IV. These results reflect the greater stoichiometry range for the former compound.

4.5. *Reduced Rutile and Magneli Phases*

From sealed tube experiments we ascertained that the M_4O_7 Magneli phase solid solution was continuous between Ti_4O_7 and $V_2Ti_2O_7$. Lattice parameters for different members of the series are given in Table IV. However, for the next highest homologue, M_5O_9, considerable difficulty was encountered in preparing single phases within the series Ti_5O_9–$V_2Ti_3O_9$, particularly as the vanadium content increased. Whereas the composition $V_{0.665}Ti_{4.335}O_9$ could be reacted to give an essentially single phase M_5O_9 by applying three separate heat treatments with intermediate grindings, the same procedure applied to $V_{1.335}Ti_{3.665}O_9$ gave a mixture of mainly M_4O_7 and M_6O_{11} with a small amount of M_5O_9. Similarly, a $V_2Ti_3O_9$ composition gave

a mixture of the two adjacent, *n*-even, homologues with just a faint trace of M_5O_9. This assemblage remained unchanged with subsequent grinding and reequilibrating. From X-ray diffraction studies on each of the three phase ($M_4O_7 + M_6O_{11} + M_5O_9$) mixtures it was found that the lattice parameters of the different Magneli phases changed with the V/(V + Ti) ratio in the bulk composition; i.e. the obtained phase assemblages shown in Table I do not indicate an equilibrium three-phase mixture, but more likely represents a series of metastable $(V,Ti)_5O_9$ phases with free energies slightly higher than those of the adjacent $(V,Ti)_4O_7$ and $(V,Ti)_6O_{11}$ phases. As both the vanadium and titanium end member M_5O_9 homologues can be prepared easily, the metastable nature of the mixed homologues must be related to the difficulty of diffusion and ordering the two different atom types within the close packed anion lattice.

We have previously observed a lower stability of *n*-odd Magneli phases relative to the *n*-even homologues in a number of related systems, notably the binary Ti_nO_{2n-1} (*3*) and the ternary systems $FeTi_{n-1}O_{2n-1}$–Ti_nO_{2n-1} (*3*) and $MnTi_{n-1}O_{2n-1}$–Ti_nO_{2n-1} (*17*). The relative stabilities may be related to the different degrees of crystallographic "freedom" that the metal atoms have in the structures. In V_5O_9, representing an *n*-odd homologue, two of the six crystallographically independent vanadium atoms are located on special positions at inversion centers (*18*), whereas in the *n*-even homologue V_4O_7, all four crystallographically independent vanadium atoms are in completely general positions (*19*). Thus, in V_5O_9 the atoms have less flexibility to adjust to metal–metal repulsions and other forces and so minimize the lattice energy than do the atoms in V_4O_7, resulting in a lower stability for the former.

For the higher Magneli phases with $n = 6$, 7 and 8 we prepared mixtures corresponding to the vanadium end members in the composition field V_2O_3–Ti_2O_3–TiO_2, i.e., the $V_2O_3 \cdot (n-2)$ TiO_2 compositions. The results, given in Table I, show that predominantly single phase products were obtained for the $n = 6$ and 8 homologues, and it is reasonable to expect complete solid solution between these phases and the titanium end members Ti_6O_{11} and Ti_8O_{15} respectively. However, as for $V_2Ti_3O_9$, the $n = 7$ composition $V_2Ti_5O_{13}$ gave a mixture of *n*-even homologues. The highest stable homologues are known to be Ti_9O_{17} in the Ti–O system (*5*) and V_8O_{15} in the V–O system (*6*).

Beyond the well-defined alternate one- and two-Magneli phase regions there exists a quasicontinuous series of reduced rutiles, MO_{2-x}, which, like the Magneli phases, may be considered as crystallographic shear (*CS*) structures based on the rutile type. The upper compositional limit for the reduced rutile phases is $TiO_{1.95}$ for the binary system (*5*), and with addition of vanadium this value drops to $\sim(V,Ti)O_{1.93}$ for a V/(V + Ti) ratio of 0.08 (interpolated from the data in Table II for the $f_{O_2} = 10^{-12.20}$ and $10^{-13.73}$ atm runs) and to $(V,Ti)O_{1.92}$ for compositions along the V_2O_3–TiO_2 join. In the binary V–O system at 1600°K, the upper limit for the reduced rutile phases has been reported as $VO_{1.905}$ (*15*).

At higher O/M ratios, the reduced rutiles are in equilibrium with rutile which has a lower stoichiometry limit of $(Ti,V)O_{1.99}$ with regard to incorporation of both V_2O_3 and Ti_2O_3 (see Table I).

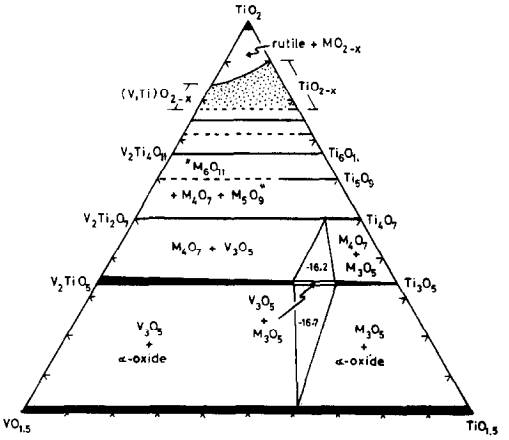

FIG. 5. Phase relations in the system V_2O_3–Ti_2O_3–TiO_2 at 1473°K. Compositions in mole percent. The numbers (–16.2 and –16.7) refer to the $\log f_{O_2}$ values for the three-phase regions, described in Table III. V_3O_5 refers to a $(V,Ti)_3O_5$ solid solution with the V_3O_5 structure.

The phase relations in the V_2O_3–Ti_2O_3–TiO_2 system are summarized in the isothermal composition section in Fig. 5.

Acknowledgments

The authors wish to thank Dr. A. G. Turnbull for help with thermodynamic computing and Ms. J. Rundle for assistance with chemical analyses and X.R.D. measurements.

References

1. *Australian Financial Review*, 30 March 1973, p. 11.
2. I. E. GREY, A. F. REID, AND D. G. JONES, *Inst. Mining Met. Trans., Sect. C* **83**, 105 (1974).
3. I. E. GREY, C. LI, AND A. F. REID, *J. Solid State Chem.* **11**, 120 (1974).
4. G. ANDERSSON, *Acta Chem. Scand.* **8**, 1599 (1954).
5. S. ANDERSSON, B. COLLEN, U. KUYLENSTIERNA, AND A. MAGNELI, *Acta Chem. Scand.* **11**, 1641 (1957).
6. S. ANDERSSON, A. SUNDHOLM, AND A. MAGNELI, *Acta Chem. Scand.* **13**, 989 (1959).
7. A. MAGNELI, S. ANDERSSON, L. KIHLBORG, S. ASBRINK, S. WESTMAN, B. HOLMBERG, AND C. NORDMARK, U.S. Dept Army Technical Report, DA-01-591-EUC-1319, Dec. 1960.
8. S. ASBRINK AND A. MAGNELI, *Acta Crystallogr.* **12**, 575 (1959).
9. S. ASBRINK, S. FRIBERG, AND A. MAGNELI, *Acta Chem. Scand.* **13**, 603 (1959).
10. G. ASBRINK, S. ASBRINK, A. MAGNELI, H. OKINAKA, K. KOSUGE, AND S. KACHI, *Acta Chem. Scand.* **25**, 3889 (1971).
11. H. OKINAKA, K. KOSUGE, AND S. KACHI, *Trans. Jap. Inst. Metals* **12**, 44 (1971).
12. R. R. MERRITT AND B. G. HYDE, *Phil. Trans. Roy. Soc. London* **274**, 627 (1973).
13. K. SUZUKI AND K. SAMBONGI, *Tetsu To Hagane* **58**, 1579 (1972).
14. A. H. WEBSTER AND N. F. H. BRIGHT, *J. Amer. Ceram. Soc.* **44**, 110 (1961).
15. T. KATSURA AND M. HASEGAWA, *Bull. Chem. Soc. Japan* **40**, 561 (1967).
16. M. W. CHASE, J. L. CURNUTT, H. PROPHET, R. A. MCDONALD, AND A. N. SYVERUD, *J. Phys. Chem. Ref. Data* **4**, 1 (1975).
17. I. E. GREY, C. LI, AND A. F. REID, *J. Solid State Chem.* **17**, 343 (1976).
18. M. MAREZIO, P. D. DERNIER, D. B. MCWHAN, AND S. KACHI, *J. Solid State Chem.* **11**, 301 (1974).
19. M. MAREZIO, D. B. MCWHAN, P. D. DERNIER, AND J. P. REMEIKA, *J. Solid State Chem.* **6**, 419 (1973).
20. W. R. ROBINSON, *Acta Crystallogr., Sect. B.* **31**, 1153 (1975).
21. S. ANDERSSON, B. COLLEN, G. KRUUSE, U. KUYLENSTIERNA, A. MAGNELI, H. PESTMALIS, AND S. ASBRINK, *Acta Chem. Scand.* **11**, 1653 (1957).